1955

Determination of the static lateral end directional derivatives of an airplane by steady flight testing

Smith, Robert P.; Vogt, Leonard F.
Lehigh University

http://hdl.handle.net/10945/14059

DETERMINATION OF THE STATIC LATERAL AND DIRECTIONAL DERIVATIVES OF AN AIRPLANE BY STEADY STATE FLIGHT TESTING

LT. ROBERT P. SMITH, USN

LT. LEONARD F. VOGT, JR., USN

DETERMINATION OF THE STATIC LATERAL
AND DIRECTIONAL DERIVATIVES OF AN
AIRPLANE BY STEADY STATE FLIGHT TESTING

Robert F. Smith
LT. USN

Leonard F. Vogt, Jr.
LT. USN

May 10, 1955

Aeronautical Engineering Report No. 302

Submitted in partial fulfillment of the requirements for the degree of Master of Science in Engineering from Princeton University, 1955.

TABLE OF CONTENTS

TABLES

FIGURES

33146

ACKNOWLEDGMENTS

The authors wish to express their gratitude to the Chairman of the Aeronautical Engineering Department, Professor Courtland D. Perkins and Asst. Professor Edward Seckel for their intense personal interest and counsel in the successful completion of this project.

They also wish to commend the Department for providing the excellent facilities for conducting this type of flight research. In particular, the authors wish to thank the airport manager, Mr. Robert Cooper, and Mr. Bart Reavis for their most essential help in the instrumentation and flight phases.

Appreciation is due to the Armament Test Division of the Naval Air Test Center at Patuxent River, Maryland, for loaning the equipment used in the flight phases of this project.

SUMMARY

An experimental investigation of a standard Navion type airplane was undertaken to determine the feasibility of using static flight test methods to find the aircraft's directional and lateral static stability derivatives. It was also desired to find the variation, if any, of these derivatives with aircraft velocity, power, and configuration. No attempt was made to determine any of the dynamic derivatives, since this type of testing is not designed to yield these derivatives directly.

With the aircraft instrumented to read rudder, aileron, sideslip and roll angles, assymetric rolling and yawing moments were introduced to determine the primary and secondary control moments. By flying straight sideslip runs with a rolling moment due to a bomb hung on the wing tip, and comparing these with runs made without the bomb, the primary aileron power is easily found. Similarly, straight sideslip runs with a target tow sleeve on one wing tip creating a yawing moment will lead to the rudder control power.

The secondary control moments can be directly determined from the steady state equations of motion, or approximated from the primary moments by the use of geometric measurements of the aircraft.

Knowing the primary and secondary control moments the basic lateral and directional static stability derivatives

are found from the equations of motion in straight sideslip runs.

The flight research program clearly indicated that this type of testing was readily adaptable to this class of aircraft. The results obtained were readily repeatable on separate flights.

Definite changes in the computed derivatives were found with the programmed speed and power conditions which pointed out the necessity of conducting this type of broad coverage flight test program.

DETERMINATION OF THE STATIC LATERAL AND DIRECTIONAL DERIVATIVES OF AN AIRPLANE BY STEADY STATE FLIGHT TESTING

INTRODUCTION

Since World War II, there has been a trend towards the use of flight testing as a means of obtaining or checking the stability derivatives of airplanes. The high cost and doubtful accuracy of results obtained from large scale, high speed wind tunnels has given impetus to this means of testing. It is the purpose of this investigation to determine the feasibility of applying some of the recently developed methods of obtaining stability derivatives to a light airplane.

To deduce an airplane's aerodynamic characteristics from a given flight test, it is usually necessary to analyze the response of the airplane to its various controls. The major methods now in use deal with the dynamic response of the airplane to its controls by either steady oscillation techniques or by transient response techniques. However, certain of the lateral stability derivatives can be obtained from non-dynamic steady responses to the airplane's controls.

The advantages of this method of testing are fairly obvious. Dynamic response techniques normally require extensive instrumentation to measure the rapid motions of the airplane. The accuracy of any determination is therefore a function of the accuracy of the instrumentation and a knowledge of the airplane's mass and complicated inertia characteristics. Steady, non-oscillatory response techniques are not susceptible to many of the inherent difficulties experienced in dynamic testing. Therefore, if the airplane is not severely limited in endurance, many of the lateral derivatives can be obtained with greater accuracy and at much less cost by these means.

In this report, the methods for obtaining and analyzing flight test curves for the static lateral stability derivatives are discussed. In particular, it deals with methods of obtaining aileron power, $C_{l_{\delta_a}}$, rudder power, $C_{n_{\delta_r}}$, secondary control moments and forces, $C_{n_{\delta_a}}$, $C_{l_{\delta_r}}$, and $C_{y_{\delta_r}}$, directional stability, C_{n_β}, dihedral effect, C_{l_β}, and side force derivative, C_{y_β}. The parameters are determined at varying speeds, power, and aircraft configurations to ascertain what variations occur.

The investigation was conducted during the spring of 1955 by Lieutenant R. P. Smith, USN and

Lieutenant L. W. Vogt, Jr., USN, while studying under the Department of Aeronautical Engineering of Princeton University, Princeton, New Jersey.

DISCUSSION OF THEORY

The equations of motion of airplane lateral dynamics, using stability (wind) axes, are

$$(C_{y_\beta} - 2D)\beta - 2D\psi + C_L\phi + C_{y_{\delta_r}}\delta_r = 0 \qquad (a)$$

$$\mu C_{l_\beta}\beta + \left(\frac{C_{l_r}}{2} + J_{xz}D\right)D\psi + \left(\frac{C_{l_p}}{2}D - J_x D^2\right)\phi$$
$$+\mu C_{l_{\delta_a}}\delta_a + \mu C_{l_{\delta_r}}\delta_r = 0 \qquad (b) \quad (1)$$

$$\mu C_{n_\beta}\beta + \left(\frac{C_{n_r}}{2} - J_z D\right)D\psi + \left(\frac{C_{n_p}}{2}D + J_{xz}D^2\right)\phi$$
$$+\mu C_{n_{\delta_a}}\delta_a + \mu C_{n_{\delta_r}}\delta_r = 0 \qquad (c)$$

In conducting steady state lateral flight testing, where $\dot{\beta} = \ddot{\psi} = \dot{\phi} = \ddot{\phi} = 0$, it is convenient to use the time derivative rather than $D\psi$, the non-dimensional yaw rate. Imposing the steady state conditions, the equations of motion become

$$C_{y_\beta}\beta - C_L\frac{V}{g}\dot{\psi} + C_L\phi + C_{y_{\delta_r}}\delta_r = 0 \qquad (a)$$

$$C_{l_\beta}\beta + C_{l_r}\frac{b}{2V}\dot{\psi} + C_{l_{\delta_a}}\delta_a + C_{l_{\delta_r}}\delta_r = 0 \qquad (b) \quad (2)$$

$$C_{n_\beta}\beta + C_{n_r}\frac{b}{2V}\dot{\psi} + C_{n_{\delta_r}}\delta_r + C_{n_{\delta_a}}\delta_a = 0 \qquad (c)$$

In these equations there are five variables $(\beta, \dot{\psi}, \phi, \delta_a, \delta_r)$.

In steady state flight testing methods particular

variables are eliminated by special flight manuevers. The three possible manuevers are the perfect turn ($\beta = 0$), the straight sideslip ($\dot{\psi} = 0$), and the skidding turn ($\phi = 0$).

The perfect turn and skidding turn maneuvers are primarily used to determine the damping derivatives C_{n_r} and C_{l_p}, and the cross derivatives C_{l_r} and C_{n_p}. These tests were not conducted.

For the straight sideslip maneuver, the equations (2) reduce to the following:

$$
\begin{aligned}
C_{y_\beta}\,\beta + C_L\,\phi + C_{y_{\delta_r}}\,\delta_r &= 0 && (a)\\
C_{l_\beta}\,\beta + C_{l_{\delta_a}}\,\delta_a + C_{l_{\delta_r}}\,\delta_r &= 0 && (b) \qquad (3)\\
C_{n_\beta}\,\beta + C_{n_{\delta_r}}\,\delta_r + C_{n_{\delta_a}}\,\delta_a &= 0 && (c)
\end{aligned}
$$

The airplane was instrumented so that the variables β, ϕ, δ_r and δ_a could be recorded and the coefficient C_L determined.

The secondary control moments are expressed in terms of the primary moments as follows:

$$C_{y_{\delta_r}} = K_1\, C_{n_{\delta_r}} \qquad K_1 = -b/l_v \qquad (4)$$

$$C_{l_{\delta_r}} = K_2\, C_{n_{\delta_r}} \qquad K_2 = -h_v/l_v \qquad (5)$$

$$C_{n_{\delta_a}} = K_3\, C_{l_{\delta_a}} \qquad (6)$$

where b is the wing span, l_v is the horizontal distance from the airplane's c.g. to the centroid of the vertical tail and h_v is the vertical distance from the airplane's

X axis to the centroid of the vertical tail.

Rewriting the equations (5), the final working form was obtained.

$$C_{y_\beta}\beta + C_L\phi + K_1 C_{n_{\delta r}}\delta_r = 0 \qquad (a)$$

$$C_{l_\beta}\beta + C_{l_{\delta a}}\delta_a + K_2 C_{n_{\delta r}}\delta_r = 0 \qquad (b) \qquad (7)$$

$$C_{n_\beta}\beta + C_{n_{\delta r}}\delta_r + K_3 C_{l_{\delta a}}\delta_a = 0 \qquad (c)$$

To determine the primary control moments, two known torques were applied to the aircraft and the control movement necessary to overcome this torque was easily converted to control power. To determine $C_{l_{\delta a}}$, the rolling moment due to aileron, a known weight was hung on the left wingtip. This introduced a known rolling moment coefficient

$$C_{l_a} = \frac{W_a \cdot y}{q\,S\,b} \qquad (8)$$

The yawing moment due to aerodynamic drag of this weight was calculated to be negligible.

In wings level flight ($\phi = 0$), the rolling equilibrium equation from (7b) and (8) is

$$C_{l_\beta}\beta + C_{l_{\delta a}}\delta_a + K_2 C_{n_{\delta r}}\delta_r + C_{l_a} = 0 \qquad (9)$$

At zero sideslip then, the ailerons must be deflected a larger angle with the introduction of C_{l_a}. For a first approximation the secondary control moment, $K_2 C_{n_{\delta r}}\delta_r$ was assumed equal to zero. Thus the aileron control power was

$$C_{l_{\delta a}} = -\frac{C_{l_a}}{\Delta\,\delta_a} \qquad (10)$$

The rudder control power $C_{n_{\delta r}}$ was determined

by introducing a known yawing moment about the airplane's Z axis and balancing it by rudder deflection.

Using a strain gage instrumented tow target sleeve attached to the wing tip, the known yawing moment was $C_{n_a} = \dfrac{D_T \cdot y}{q S b}$ (11)

The yawing equilibrium equation became

$$C_{n\beta}\beta + C_{n_{\delta r}}\delta_r + K_3 C_{l_{\delta a}}\delta_a + C_{n_a} = 0 \qquad (12)$$

Test data at zero sideslip, sleeve on and off, gave the difference of rudder deflection required. Considering as a first approximation that the aileron adverse yaw, $K_3 C_{l_{\delta a}}\delta_a$, was zero, the rudder power was

$$C_{n_{\delta r}} = -\frac{C_{n_a}}{\Delta\delta_r} \qquad (13)$$

Returning to the assymetric weight test, the difference of rudder angles required for trim between weight on and off is due to the yawing moment of the additional aileron deflection. From equation (7c)

$$C_{n\beta}\beta + C_{n_{\delta r}}\delta_r + K_3 C_{l_{\delta a}}\delta_a = 0$$

can now be solved for K_3, thus:

$$K_3 = -\frac{C_{n_{\delta r}}}{C_{l_{\delta a}}} \cdot \frac{\Delta\delta_r}{\Delta\delta_a} \qquad (14)$$

Iteration of the coefficients $C_{l_{\delta a}}$, $C_{n_{\delta r}}$ and of K_3 was used to obtain the most accurate answers for the data collected by the following equations:

$$C_{l_{\delta a}} = \frac{-C_{l_a} - K_2 C_{n_{\delta r}}\Delta\delta_r}{\Delta\delta_a} \qquad (15)$$

$$C_{n_{\delta r}} = \frac{-C_{n_a} - K_3 C_{l_{\delta a}}\Delta\delta_a}{\Delta\delta_r} \qquad (16)$$

Finally, the three secondary control moments

$C_{y\delta_r}$, $C_{l\delta_r}$ and $C_{n\delta_a}$ can be obtained from equations (4), (5), and (6).

Knowing the primary and secondary control moment coefficients, the static lateral stability derivatives, $C_{y\beta}$, $C_{l\beta}$ and $C_{n\beta}$, were determined from the straight side-slip equations (7a), (7b), and (7c). The slopes of the flight test data curves through zero sideslip are used in the following equations to determine the static lateral and directional derivatives.

$$C_{y\beta} = -C_L \frac{d\phi}{d\beta} - K_1 C_{n\delta_r} \frac{d\delta_r}{d\beta} \qquad (a)$$

$$C_{l\beta} = -C_{l\delta_a} \frac{d\delta_a}{d\beta} - K_2 C_{n\delta_r} \frac{d\delta_r}{d\beta} \qquad (b) \quad (17)$$

$$C_{n\beta} = -C_{n\delta_r} \frac{d\delta_r}{d\beta} - K_3 C_{l\delta_a} \frac{d\delta_a}{d\beta} \qquad (c)$$

EQUIPMENT AND PROCEDURES

The test vehicle used to obtain flight data was a Ryan Navion, N5113K. This is a four-place transport powered by a 205 HP Continental engine. The aircraft was standard in configuration except for the modifications made for these tests, and is pictured in Figs. 1, 2 and 3.

In order to mount the equipment required to place known rolling and yawing moments on the aircraft, two steel lugs were fastened to the outermost stiffening rib of each wing. To each of these a standard U. S. Navy Mark 8 bomb shackle was attached. These shackles are manually operated

and were activated by steel cables led through the wing to the cockpit (Fig. 3).

A boom with a yaw vane attached was mounted so as to extend forward from the left wingtip lugs (Fig. 1). Movement of the vane energized an autosyn transmitter mounted within a streamlined shape. This boom was sufficiently long so that it was logical to assume that the vane was not affected by the aircraft pressure field. Another boom extended aft from the right wing tip lugs. This was used to support the equipment required to give a known yawing moment. Fig. 3 shows this arrangement.

For the series of tests designed to measure $C_{l_{\delta a}}$, a "bomb", actually a streamlined shape made of stock steel, was carried on each bomb shackle for takeoff. Although these bombs weighed approximately 80 pounds each, no undue stress concentration was noticed during takeoff or during any maneuvers. After takeoff, the right bomb was dropped, and a series of tests made with the known weight (78 lbs., 5 ozs.) on the left wingtip. (All takeoffs and landings were made with symmetrical loads since there was some doubt if the aircraft would have sufficient aileron power at low speeds in the unbalanced condition. It is felt that this was unnecessary.) Then the bomb on the left wingtip was dropped and the same tests made in the clean configuration. In this way, duplication of atmospheric conditions was obtained.

To determine $C_{n_{\delta_r}}$, a standard U. S. Navy Mark 23, Mod C, 20 foot tow target sleeve was towed behind the right wingtip. Originally, takeoffs were made by stretching 450 feet of nylon line, with the sleeve attached, ahead of the airplane. A maximum performance takeoff was made and the target "snatched" into the air. Power limitations of the aircraft coupled with the roughness and short length of the field precluded any successful "snatches" without approximately 10 knots of headwind.

These limitations finally caused a redesign of the system to that shown in Fig. 2. In this system, the target was fastened to the rear of the fuselage with 150 feet of line and the remainder of the line looped from the tail to the wingtip. After takeoff and climb out, the tail attachment point was released and the target supported by the wingtip.

Some difficulty was experienced on several test flights when the tow target started to oscillate and rotate. The only apparent cause was that the target was in the wing vortex trail. By placing a five pound weight on the target support ring, this difficulty was alleviated.

To measure the drag of the target a strain gage unit was designed and placed directly aft of the boom. Electrical wires were led through the wing structure and readings made on a Baldwin SR-4 strain gage box in the cockpit. Immediately aft of the strain gage a "pelican" type

release hook was attached with an activating cable led into the cockpit. The target was released prior to landing and on all unsuccessful "snatches". Fig. 3 shows the right wingtip arrangement. It was found absolutely essential to have a dependable bearing in the line to take out any twist caused by rotation of the target in the air. Once again the same tests were run in the clean configuration in order to duplicate atmospheric conditions.

To measure control deflections one autosyn transmitter was mounted on the rudder surface and another on the aileron control cable. This equipment was ground calibrated. It is interesting to note that only differences and slopes of all measured quantities were used in the computations. Therefore it was not necessary to determine accurately the zero points of control deflections or sideslip indications. A standard double needle autosyn receiver-indicator was mounted in the cockpit and with suitable step-up pulleys, large indicator deflections were obtained for small control deflections.

Since these tests were being conducted concurrently with another series on the aircraft, sideslip indications were obtained by converting the autosyn transmitter output to a direct current voltage. Readings were then made on a direct current voltmeter.

A standard inclinometer was mounted in the cockpit

perpendicular to the roll axis of the aircraft in order to read roll angle. With proper shock mounting to damp out high frequency vibrations, this gave very satisfactory results.

Even though the primary purpose of this investigation was to determine the feasibility of obtaining certain of the lateral and directional stability derivatives by static flight test means, the variation of these derivatives with aircraft speed, power, and flap deflection was also desired. To accomplish this end, seven series of tests were made. With power for level flight, tests were made at 80, 100, and 120 miles per hour. For the three tests made at each speed, i.e. assymetric weight, assymetric drag, and clean, the engine speed was held constant, 1800 rpm for 80 mph, 1900 rpm for 100 mph, and 2000 rpm for 120 mph. The same series of tests were then conducted at 80, 100 and 120 mph with maximum continuous power applied. For this aircraft maximum continuous power is listed as 25 inches manifold pressure and 2300 rpm. In these tests of course, the aircraft climbed. In addition, a series of tests were made at maximum continuous power with full flap deflection. Results of all tests are shown on Fig. 4 through Fig. 17.

In all configurations, the data desired was δ_a, δ_r, and ϕ at various angles of sideslip, β. The best method to

obtain data was to deflect the rudder and stop the aircraft from turning by deflecting the aileron. Then readings were taken. In addition drag readings from the strain gage box were taken for the runs when the target was being towed. Straight flight was maintained by constant reference to the directional gyro.

DISCUSSION OF RESULTS

The data obtained from the seven different test conditions was plotted in Figs. 4 through 17, and results computed from these curves were listed in Table II. As the analysis of results was identical in all seven configurations, only the power for level flight run at 100 mph will be discussed in detail.

At $V_i = 100$ mph, q was found using the aircraft position error charts to be 27.7 lbs. per sq. ft., C_L was .519 and h_v was 2.3 ft.

From equation (8), $C_{l_a} = -.00769$. Equation (11) gave a value for $C_{n_a} = .00971$.

Using equation (10) and an aileron deflection at zero sideslip from Fig. 6 of 3.6°, the aileron control power $C_{l_{\delta a}} = -.124$.

From equation (12) and Fig. 7, the first approximation of the rudder control power was $C_{n_{\delta r}} = -\frac{.00971}{4.8/57.3} = -.116$.

Now the proportionality factor K_3 could be computed by equation (13), using the control deflections at zero sideslip thus:

$$K_3 = -\frac{-.116}{.124} \cdot \frac{-.4}{3.6} = -.104.$$

Iteration of these coefficients by equations (14), (15), and (13) produced the following final values:

$C_{l_{\delta a}} = .124$

$C_{n_{\delta r}} = -.119$

$K_3 = -.107$

From equations (4), (5) and (6) the three secondary control moments were found to be

$C_{y_{\delta r}} = -.236$

$C_{l_{\delta r}} = .0166$

$C_{n_{\delta a}} = -.0138$

Finally, using the roll angle, rudder angle and aileron angle slopes from Fig. 6, the static lateral derivatives for $V_1 = 100$ mph were determined from equations (17a), (17b) and (17c).

$C_{y_\beta} = -.546$

$C_{l_\beta} = -.0865$

$C_{n_\beta} = .144$

Examination of the results in Table II shows the variations in the computed values of the primary control powers, secondary control powers and stability derivatives with the change in speed and power conditions. These variations are to be expected and the influencing factors

are detailed below. The limiting accuracy in these calculations was felt to be the inherent inaccuracy involved in measuring and recording flight test data, then subsequently fairing curves and attempting to read control deflection differences closer than 0.1°. In particular, the aileron deflection measuring system was attached at the control column and thus no accurate account could be taken of cable stretch even though attempts were made to "load" the ailerons during the ground calibrations.

Table II and Fig. 18 show that $C_{l_{\delta a}}$ decreases as speed increases. Since aileron control cable stretch would increase as dynamic pressure increased, this could partially contribute to the reduction in aileron power at higher speeds. The normal lessening of aileron power as C_L decreases and any wing twist at higher speeds would also account for some of the noted reduction in $C_{l_{\delta a}}$.

From Table II and Fig. 18 $C_{n_{\delta r}}$ is seen to decrease with an increase in velocity. Since the rudder lies within the slipstream, this would be expected. As forward speed is increased, the effect of the slipstream decreases, and less force is exerted by the rudder per degree of deflection.

$C_{l_{\delta r}}$ is a function of $C_{n_{\delta r}}$ and might therefore be expected to decrease as velocity increases. However, as velocity increases the angle of attack decreases. This will increase h_v and from equation (5), $C_{l_{\delta r}}$ would be increased.

The aileron adverse yaw, $C_{n_{\delta a}}$ is seen to decrease

with speed. Aileron adverse yaw is partially the result of the increase in induced drag which accompanies the increase in lift of the wing when the aileron is deflected downward. Since induced drag is a function of C_L^2 it is expected that it would tend to decrease as velocity increases.

The side force derivative, C_{y_β} , should theoretically stay constant with changes in speed. The minor variations noted in Table II and Fig. 19 could possibly be caused by changes in the interference and sidewash effects of the fuselage and slipstream as speed is changed. This would affect the angle of attack of the vertical tail differently at the different speeds and power conditions.

Directional stability, C_{n_β} is almost exclusively determined by the vertical tail. Since the vertical tail lies within the slipstream, C_{n_β} would be expected to decrease as slipstream becomes less effective, i.e. as speed increases. This was noted in Table II and Fig. 19. Comparing C_{n_β} at the same speed and different power settings, Table II shows that the directional stability is reduced slightly, as power is increased. This might be explained by the fact that tractor propellers are destabilizing as the power is increased.

As expected, dihedral effect, C_{l_β} , is seen to change very little with velocity. A possible reason for the small decrease in C_{l_β} as power is increased at constant speed is that the added slipstream due to the power acts over one wing more than the other as the aircraft is sideslipped.

This introduces a rolling moment which would decrease the magnitude of C_{l_β}.

It is difficult to explain the variations seen in Table II and on Figs. 18 and 19 in the computed values of the several derivatives when the flaps were deflected. Some of the variations can be rationalized however, and these will be discussed. Since the flaps tend to interfere with the flow of the propeller slipstream over the vertical tail, the reduction in $C_{n_{\delta_r}}$, is to be expected even though the speed is lower. The minor variation of $C_{l_{\delta_a}}$ from what would be expected at low speed is not explainable.

The flap hinge line on the test aircraft was swept forward a small amount. This would partially account for the increase in the magnitude of C_{y_β} and the decrease in C_{l_β}. The interference of the deflected flaps with the slipstream would also indicate a decreased value of C_{n_β} from clean condition.

A refinement in the method of solution for primary and secondary control moments could have been used if an accurate determination of yawing moment of the weight and rolling moment of the sleeve had been made. In this project, bomb drag was calculated and found to be negligible. Rolling moment of the sleeve could be found if an accurate determination of the angle between the tow line and the aircraft's X axis (Horizon) were made.

Then from equation (3)(b) and (8), repeated here

$$C_{l_\beta}\beta + C_{l_{\delta a}}\delta_a + C_{l_{\delta r}}\delta_r = 0 \qquad (3b)$$

$$C_{l_a} = \frac{W_a}{q} \cdot \frac{y}{S\,b} \qquad (8)$$

two difference equations at zero sideslip could be written:

$$C_{l_{\delta a}}\Delta\delta_{a_{BOMB}} + C_{l_{\delta r}}\Delta\delta_{r_{BOMB}} + C_{l_{a_{BOMB}}} = 0 \qquad (18)$$

$$C_{l_{\delta a}}\Delta\delta_{a_{SLEEVE}} + C_{l_{\delta r}}\Delta\delta_{r_{SLEEVE}} + C_{l_{a_{SLEEVE}}} = 0 \qquad (19)$$

The first approximation of $C_{l_{\delta r}}\Delta\delta r_B$ would give an identical answer for $C_{l_{\delta a}}$ as the method used in this report. However, with an accurate control deflection measuring system and the above mentioned moments, it was felt that simultaneous solution of these equations would provide a more accurate determination of $C_{l_{\delta r}}$ which would not depend on the questionable measured values of h_v and l_v.

Similarly equations (3)(c) and (11) can be written as difference equations at zero sideslip.

$$C_{n_{\delta r}}\Delta\delta_{r_{BOMB}} + C_{n_{\delta a}}\Delta\delta_{a_{BOMB}} + C_{n_{BOMB}} = 0 \qquad (20)$$

$$C_{n_{\delta r}}\Delta\delta_{r_{SLEEVE}} + C_{n_{\delta a}}\Delta\delta_{a_{SLEEVE}} + C_{n_{SLEEVE}} = 0 \qquad (21)$$

Solution of these equations gives $C_{n_{\delta r}}$ and $C_{n_{\delta a}}$ without the iteration procedure previously used.

It was felt that static flight testing procedures are easily accurate enough to justify this method of solution.

CONCLUSIONS

The flight testing required for this method of determination of the static lateral and directional stability derivatives is relatively easy to perform.

The primary and secondary aileron and rudder control moments are determined directly by the flight tests.

Instrumentation necessary to obtain required flight test data is not complex and is readily available.

Reduction of flight test data and the computations necessary to extract the stability derivatives are fast and straightforward.

The directional stability and effective dihedral were found to change markedly with aircraft velocity. For the aircraft tested, there was a distinct decrease in C_{n_β} and C_{l_β} as speed increased. Therefore, it is recommended that an aircraft always be tested at various speeds and in its different configurations.

References

1. Perkins, C. D. and Hage, Robert E., "Airplane Performance Stability and Control", John Wiley and Sons, 1949.
2. Perkins, C. D., "Methods for Obtaining Aerodynamic Data Through Steady State Flight Testing, Part II, The Lateral Derivatives", C. D. Perkins, 1950.

TABLE I

DESCRIPTION OF SYMBOLS

V	Airplane velocity f.p.s.
S	Wing area (sq. ft.)
b	Wing span (ft.)
l_v	Length c.g. to vertical tail centroid (ft.)
h_v	Vertical tail centroid to X axis (ft.)
C_L	Airplane Lift coefficient
q	Dynamic pressure (lbs./sq. ft.)
C_y	Side force coefficient Y/qs
C_l	Rolling moment coefficient L/qsb
C_n	Yawing moment coefficient N/qsb
μ	Airplane relative density $m/\rho sb$
D	Differential operator $d/d(t/\tau)$
β	Sideslip angle
ψ	Yaw angle
ϕ	Bank angle
δ_r	Rudder angle
δ_a	Aileron angle (average)
C_{y_β}	Side force derivative $\partial C_y/\partial \beta$ (per radian)
C_{n_β}	Directional stability derivative $\partial C_n/\partial \beta$ (per radian)
C_{l_β}	Dihedral effect $\partial C_l/\partial \beta$ (per radian)

TABLE II

	Level Flight Power			Maximum Continuous Power			
	1800RPM	1900RPM	2000RPM	2300RPM	2300RPM	2300RPM	2300RPM FF
V_i	80	100	120	80	100	120	70
q	17.7	27.7	37.9	17.7	27.7	37.9	13.6
$C_{l_{a_{Bomb}}}$	-.01204	-.00769	-.00567	-.01204	-.00769	-.00567	-.01568
$C_{n_{a_{Sleeve}}}$	.01150	.00971	.00897	.01150	.00971	.00897	.01060
C_L	.811	.519	.390	.811	.519	.390	1.06
$\Delta\delta_{a_{Bomb}}$	4.7°	3.6°	3.2°	4.3°	3.5°	2.9°	7.8°
$\Delta\delta_{r_{Bomb}}$	1.5°	0.4°	0.1°	1.2°	0.9°	0.4°	0.7°
$\Delta\delta_{r_{Sleeve}}$	4.6°	4.8°	4.8°	4.9°	5.6°	5.7°	5.5°
$\Delta\delta_{a_{Sleeve}}$	0.8°	1.1°	0.8°	0.8°	0.8°	1.0°	0.6°
$C_{l_{\delta_a}}$	.152	.124	.101	.164	.129	.100	.115
$C_{n_{\delta_r}}$	-.151	-.119	-.107	-.140	-.105	-.0925	-.112
K_3	-.318	-.107	-.032	-.[illegible]37	-.209	-.124	-.087
$C_{l_{\delta_r}}$	.0130	.0166	.0166	.0119	.0141	.0143	.0152
$C_{n_{\delta_a}}$	-.0561	-.0138	-.0032	-.0388	-.0270	-.0124	-.0100
$C_{y_{\delta_r}}$	.291	.236	.203	.266	.200	.176	.213
$d\phi/d\beta$	.39	.58	.87	.44	.61	.87	.46
$d\delta_r/d\beta$	.98	1.14	1.30	1.17	1.16	1.39	1.28
$d\delta_a/d\beta$	.47	.55	.57	.48	.49	.56	.13
C_{y_β}	-.616	-.546	-.595	-.671	-.551	-.560	-.760
C_{l_β}	-.0905	-.0865	-.0822	-.0957	-.0814	-.0736	-.0344
C_{n_β}	.181	.144	.141	.180	.140	.118	.144

Fig. 1 Test Aircraft Showing Bombs

Fig. 2 Test Aircraft Showing Tow Target Sleeve

Fig. 3 Detail of Right Wingtip

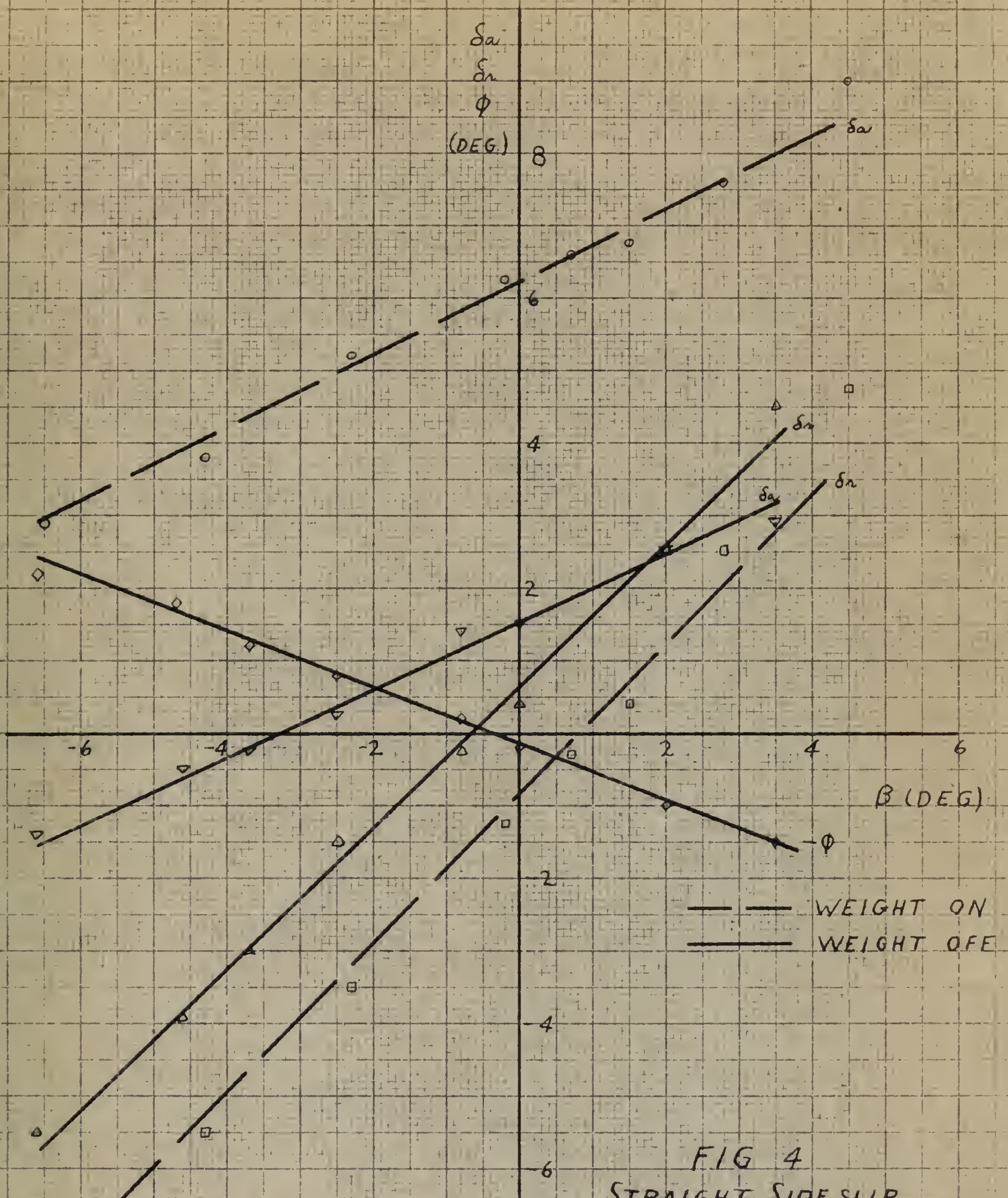

FIG 4
STRAIGHT SIDESLIP
ASSYMETRIC WEIGHT
ON LEFT WING
V = 80 MPH (LEVEL FLIGHT POWER)

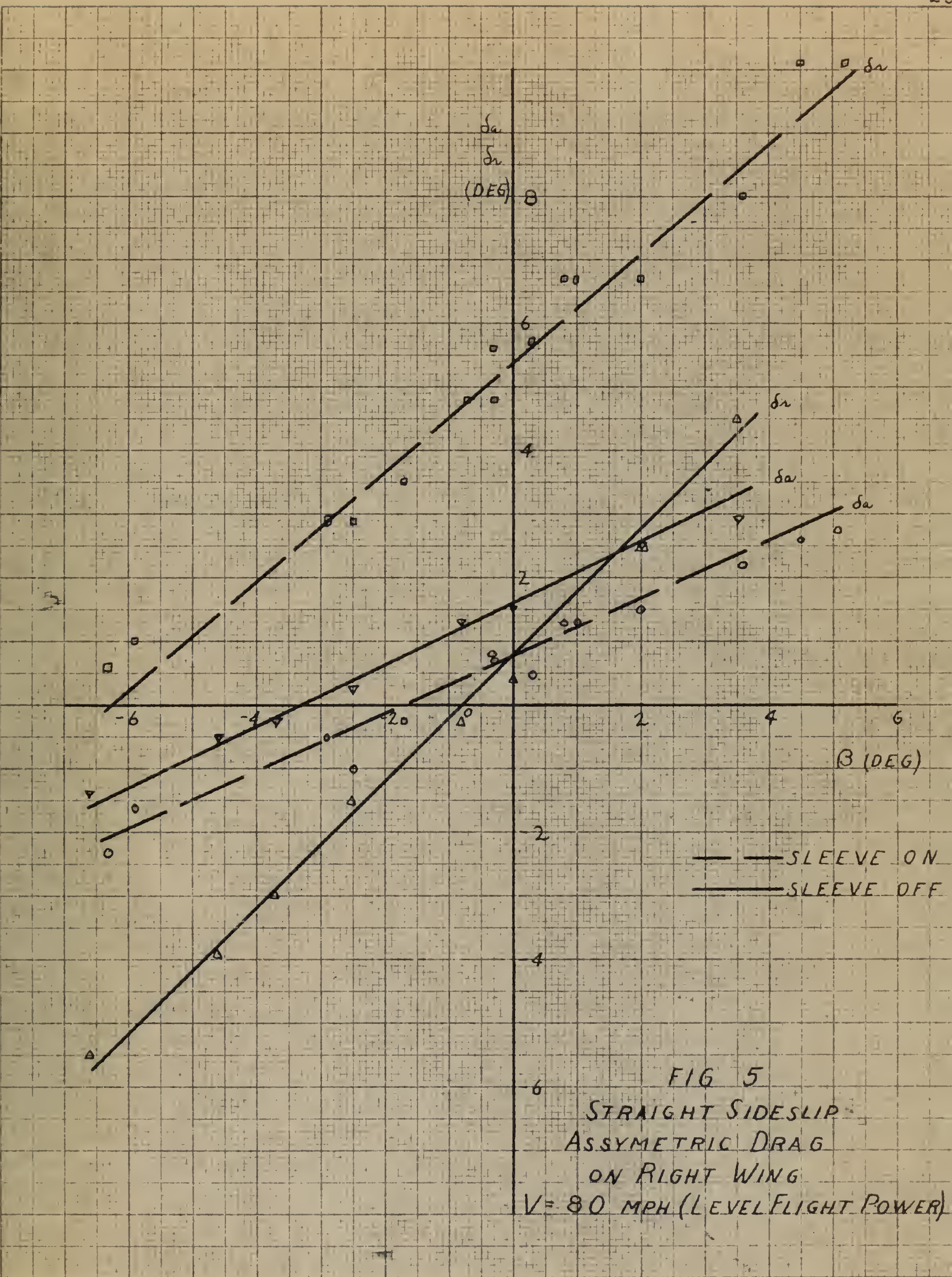

FIG 5
STRAIGHT SIDESLIP
ASSYMETRIC DRAG
ON RIGHT WING
V = 80 MPH (LEVEL FLIGHT POWER)

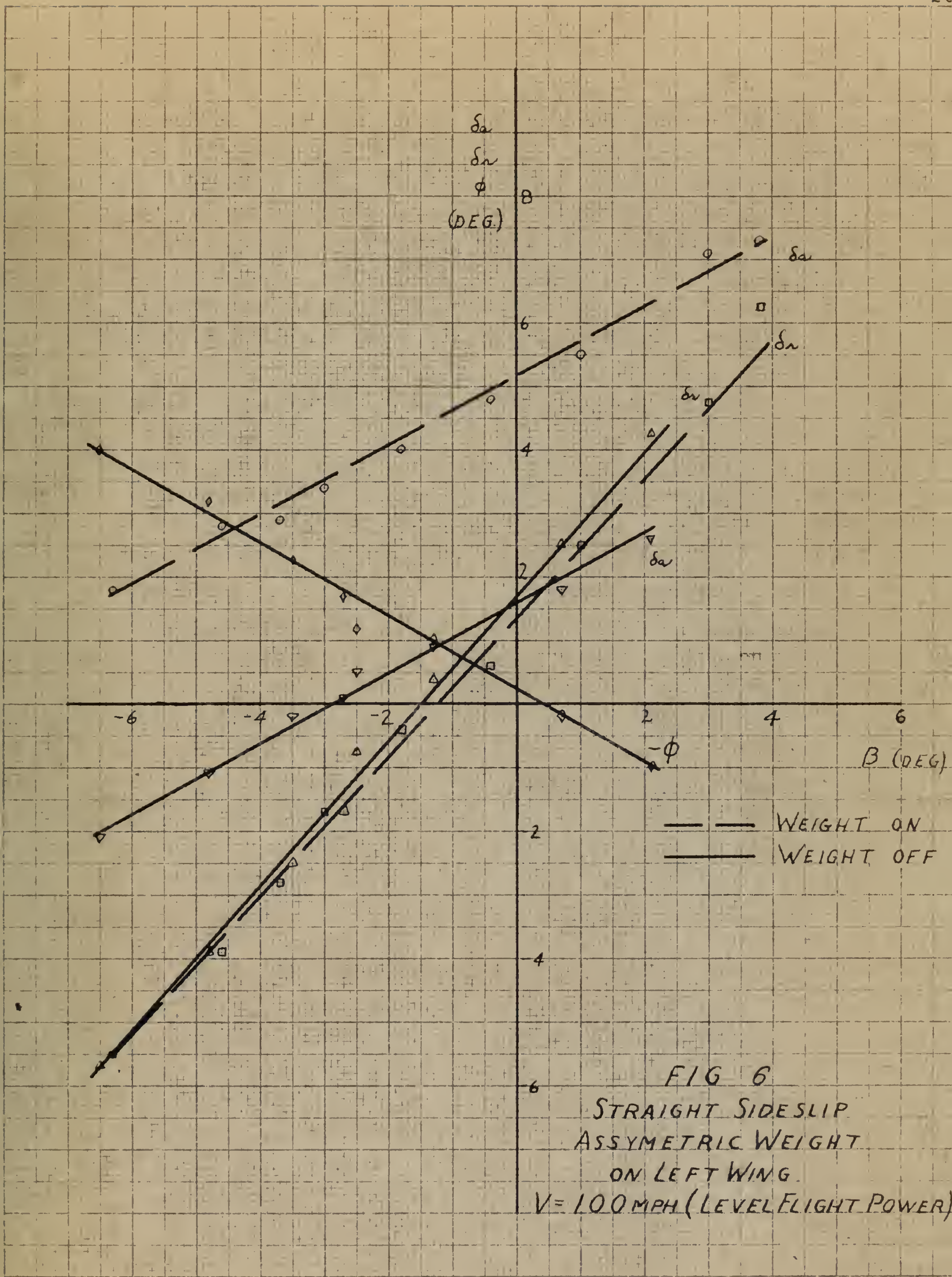

FIG 6
STRAIGHT SIDESLIP
ASSYMETRIC WEIGHT
ON LEFT WING
V = 100 MPH (LEVEL FLIGHT POWER)

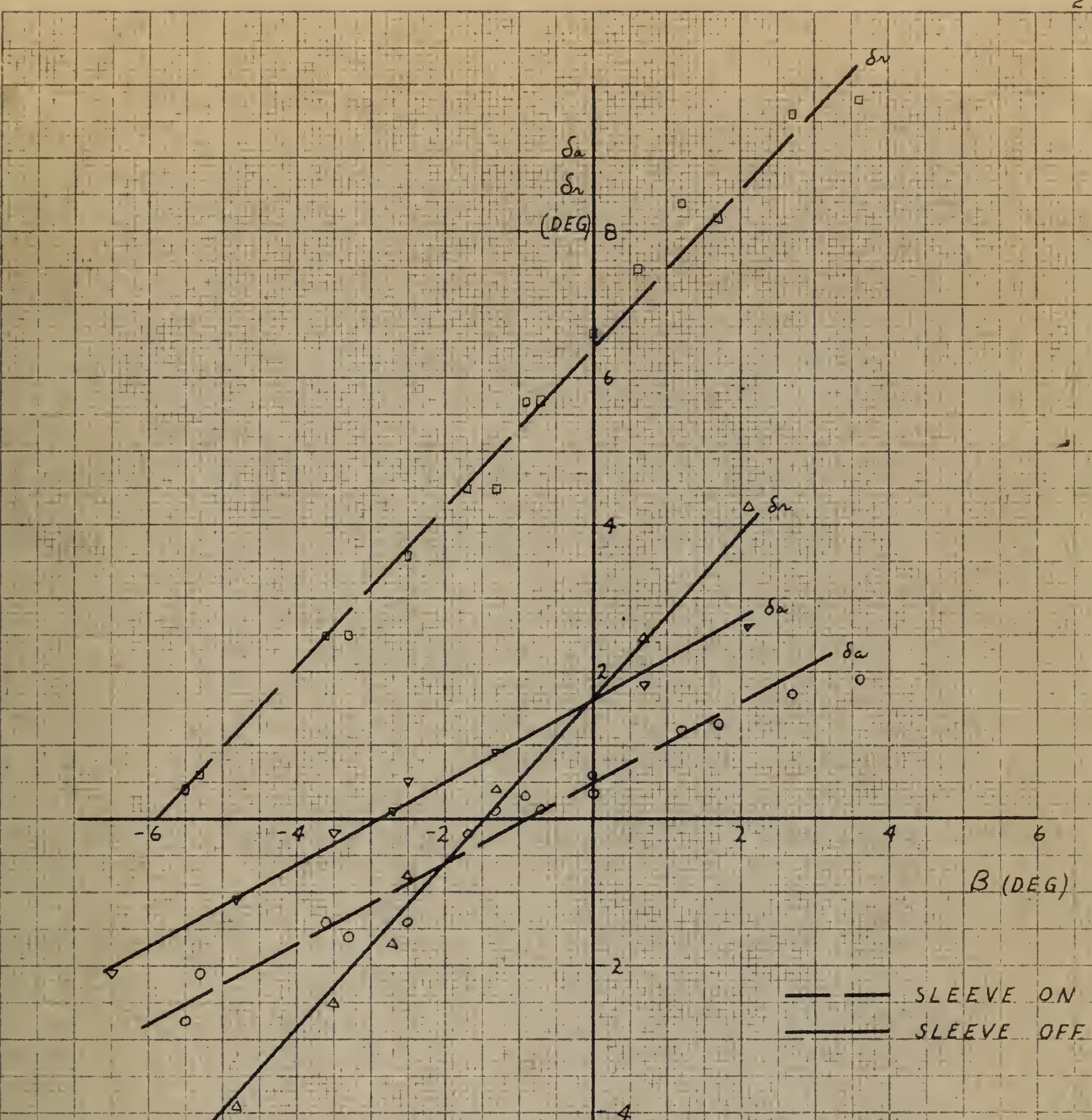

FIG 7
STRAIGHT SIDESLIP
ASSYMETRIC DRAG
ON RIGHT WING
V = 100 MPH (LEVEL FLIGHT POWER)

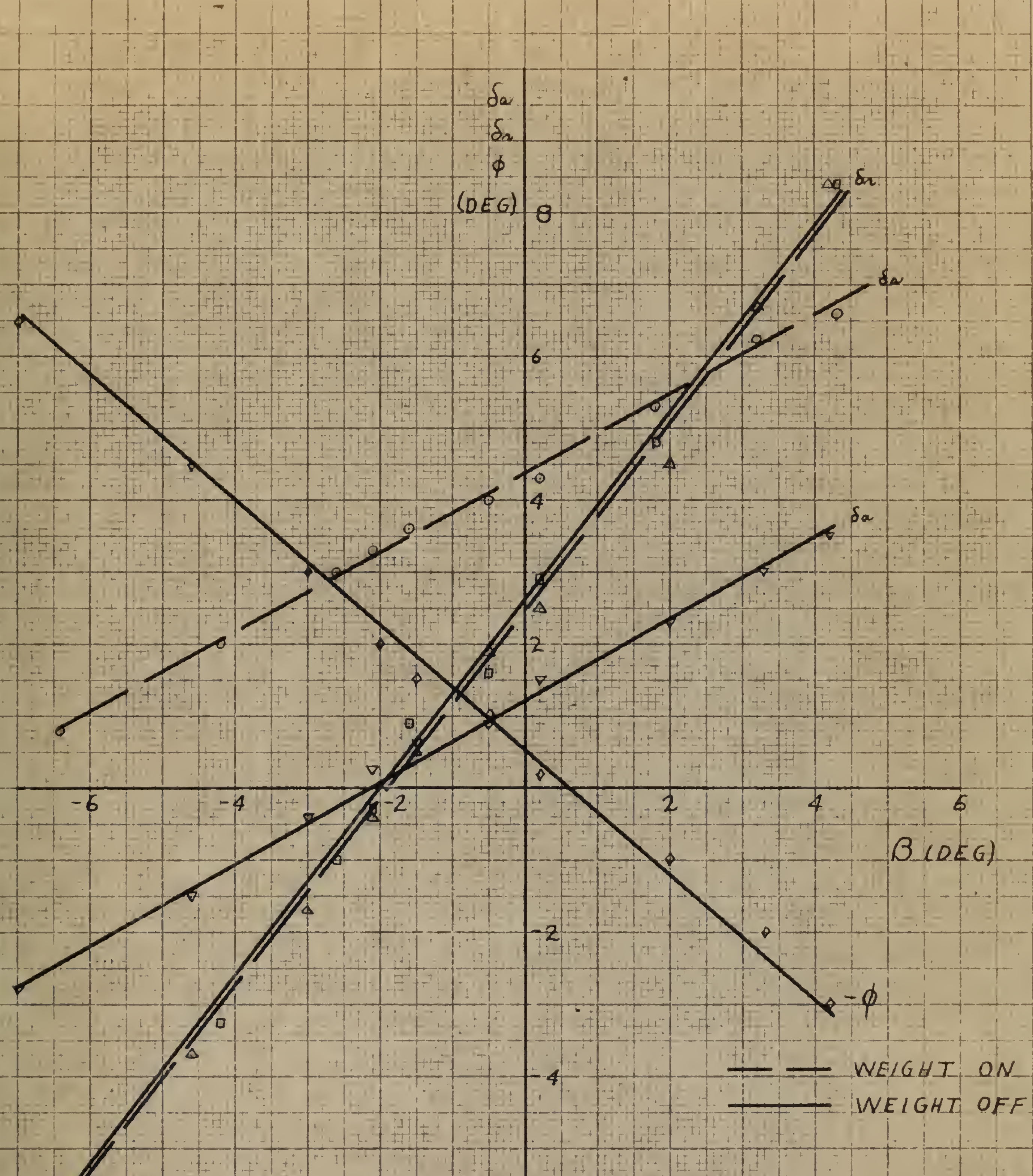

FIG 8
STRAIGHT SIDESLIP
ASSYMETRIC WEIGHT
ON LEFT WING
V=120 MPH (LEVEL FLIGHT POWER)

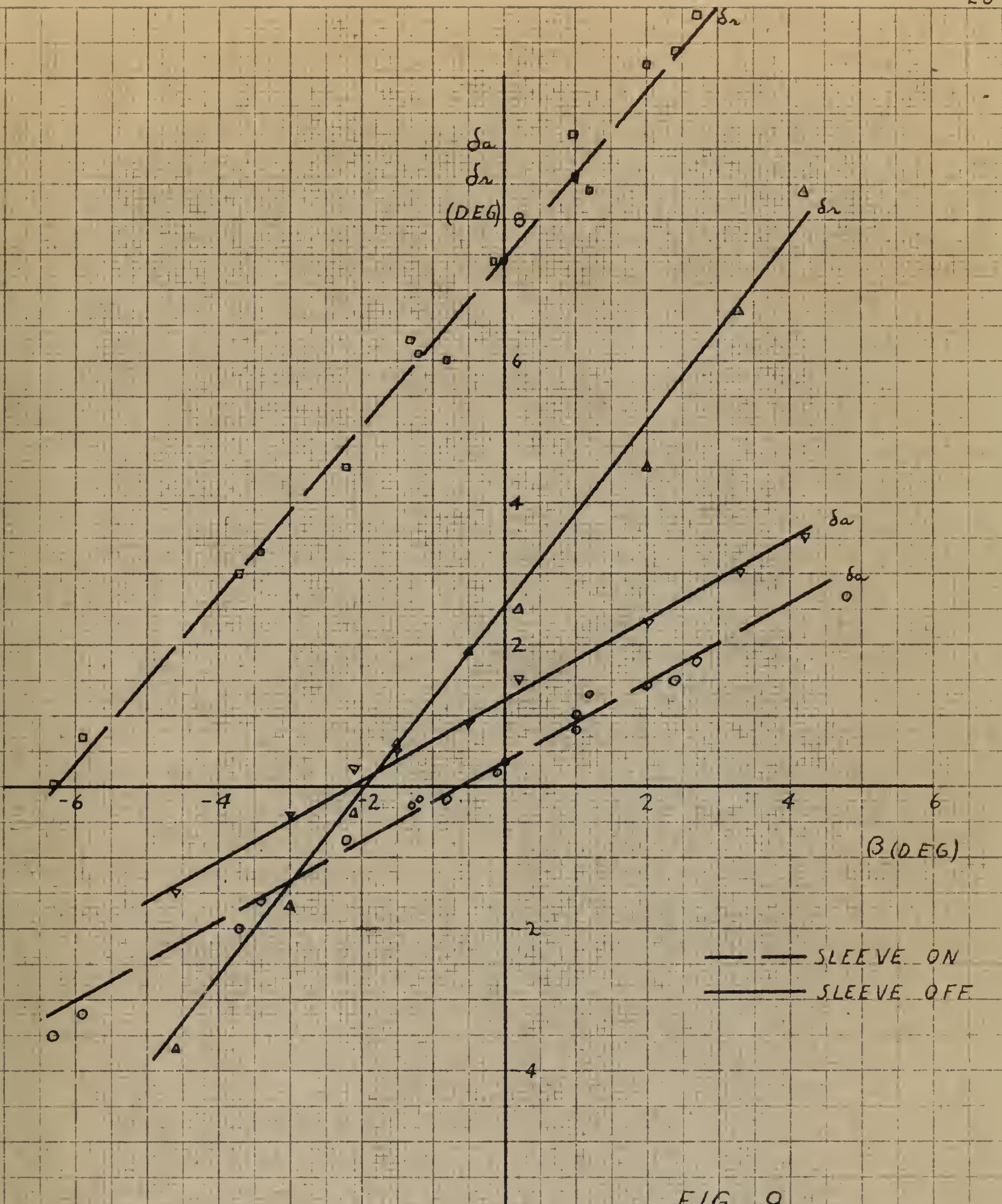

FIG. 9
STRAIGHT SIDESLIP
ASSYMETRIC DRAG
ON RIGHT WING
V = 120 MPH (LEVEL FLIGHT POWER)

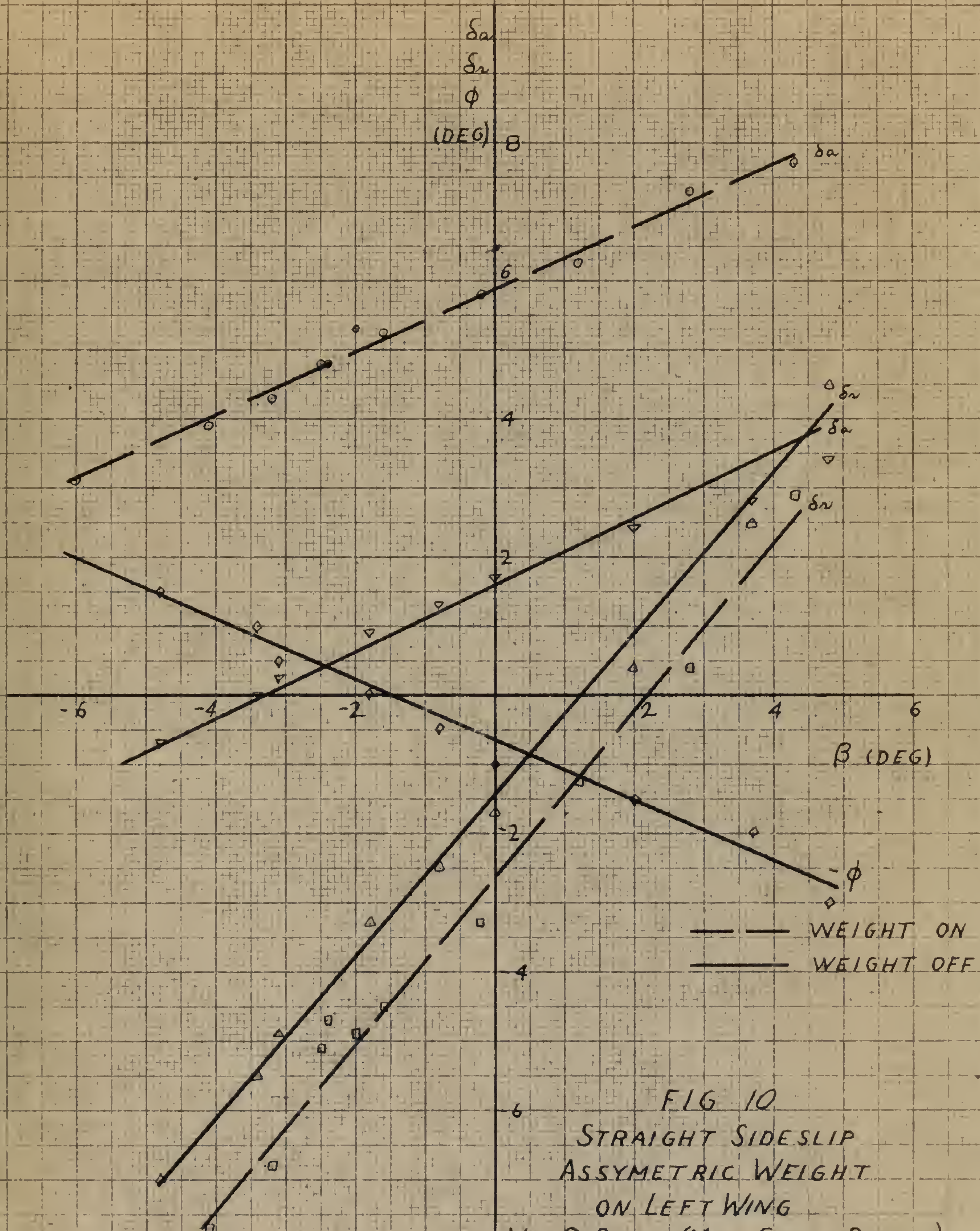

FIG 10
STRAIGHT SIDESLIP
ASSYMETRIC WEIGHT
ON LEFT WING
V = 80 MPH (MAX CONT POWER)

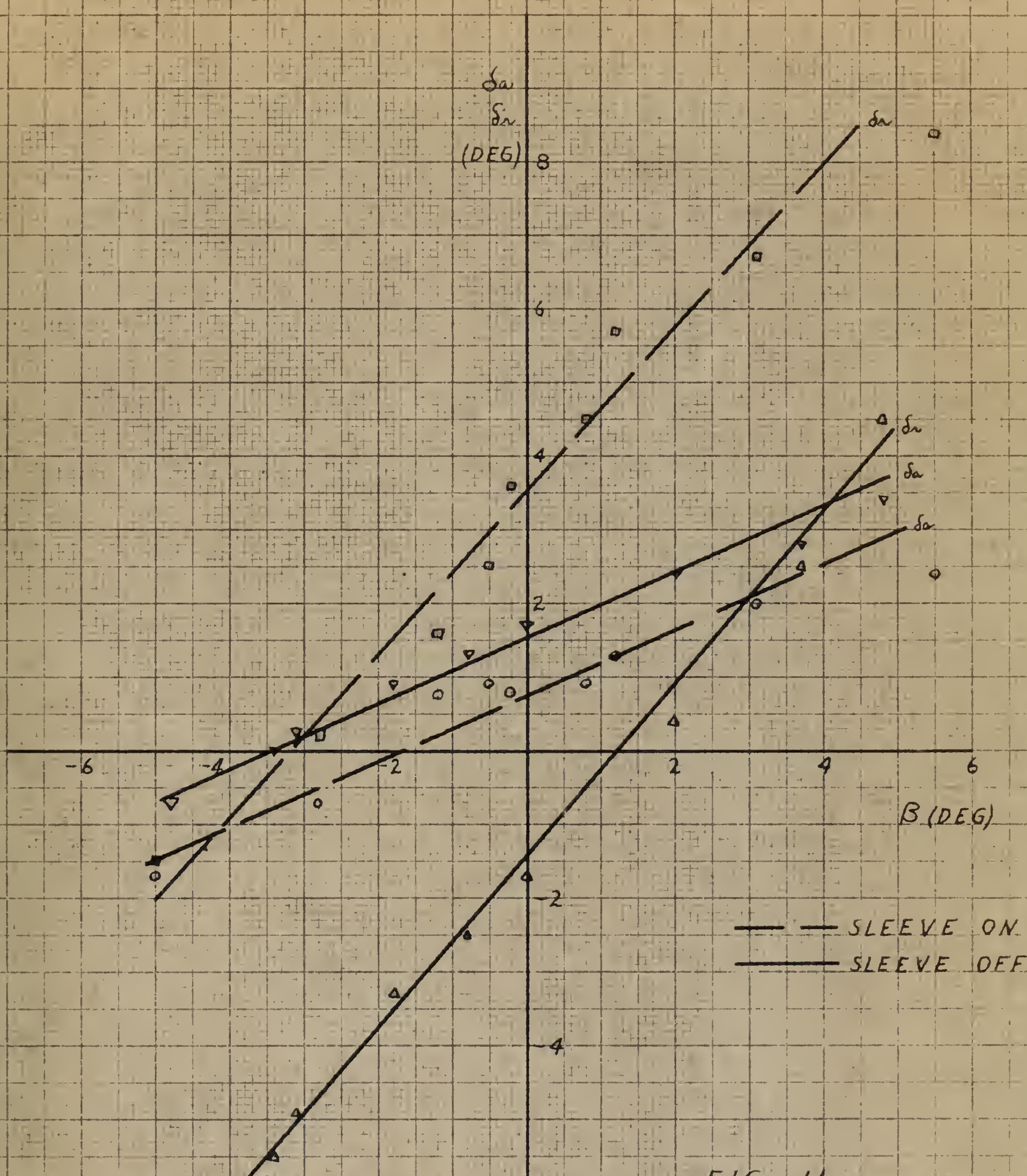

FIG 11
STRAIGHT SIDESLIP
ASSYMETRIC DRAG
ON RIGHT WING
V = 80 MPH (MAX. CONT. POWER)

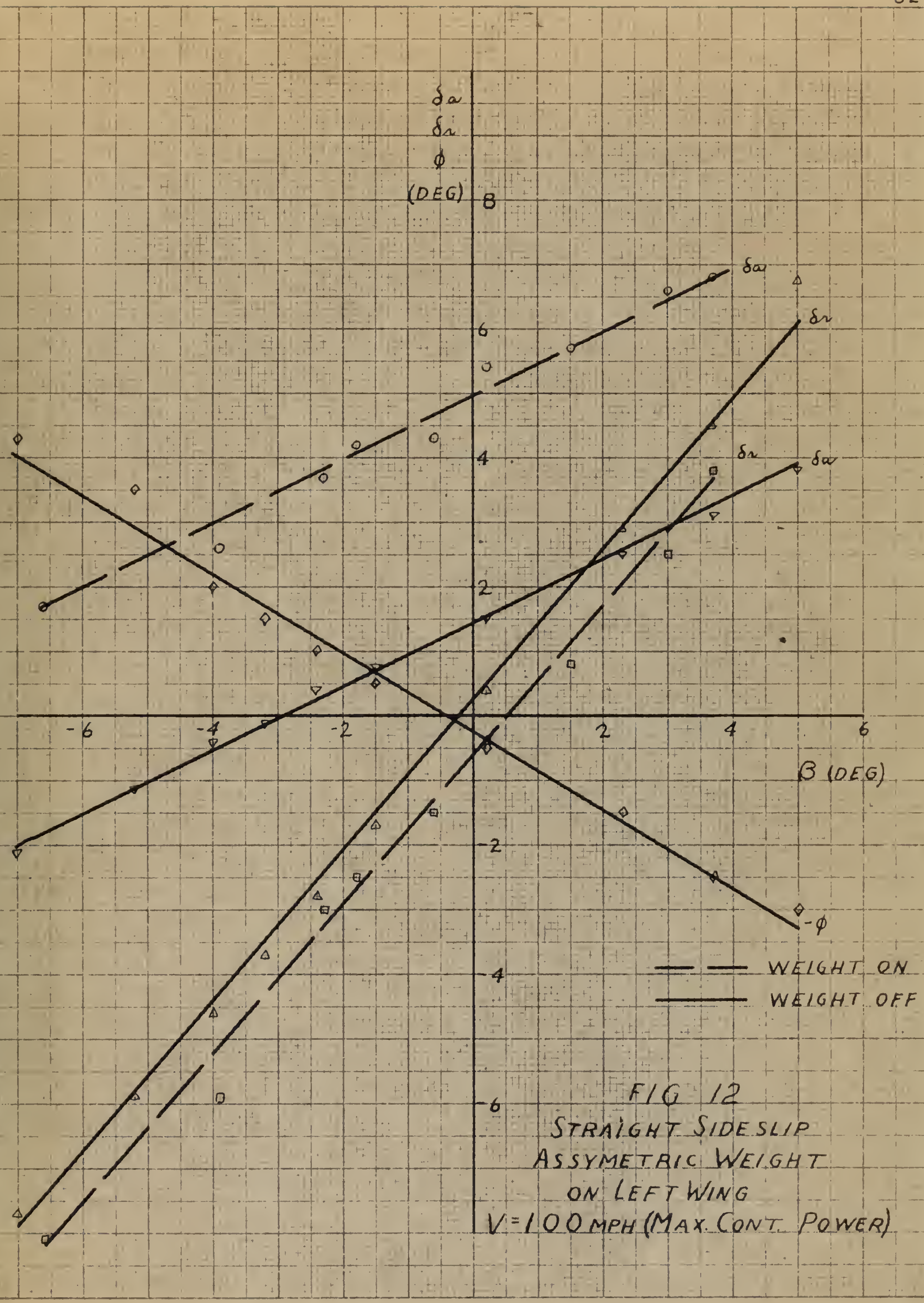

FIG 12
STRAIGHT SIDESLIP
ASSYMETRIC WEIGHT
ON LEFT WING
V=100 MPH (MAX. CONT. POWER)

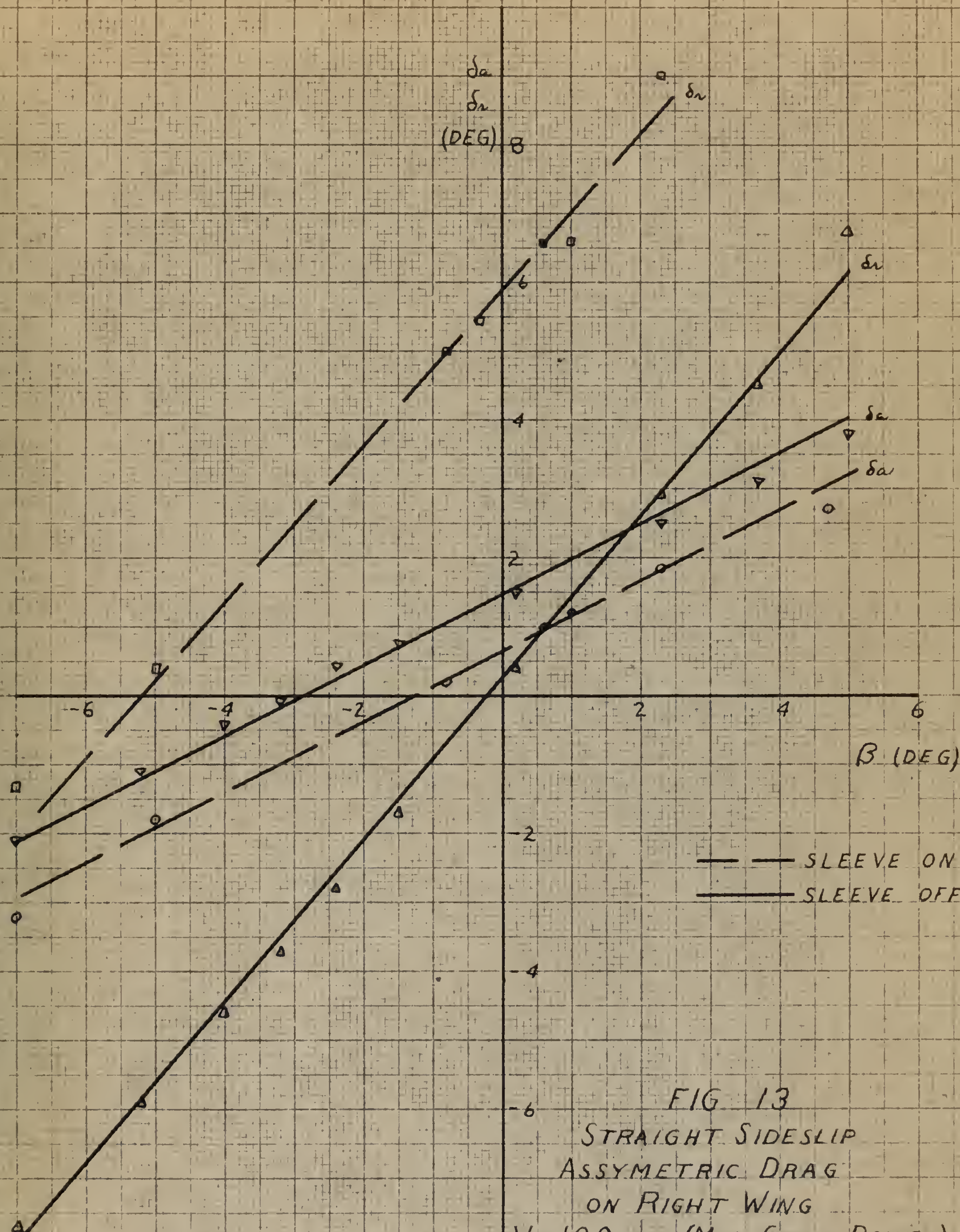

FIG 13
STRAIGHT SIDESLIP
ASSYMETRIC DRAG
ON RIGHT WING
V = 100 MPH (MAX. CONT. POWER)

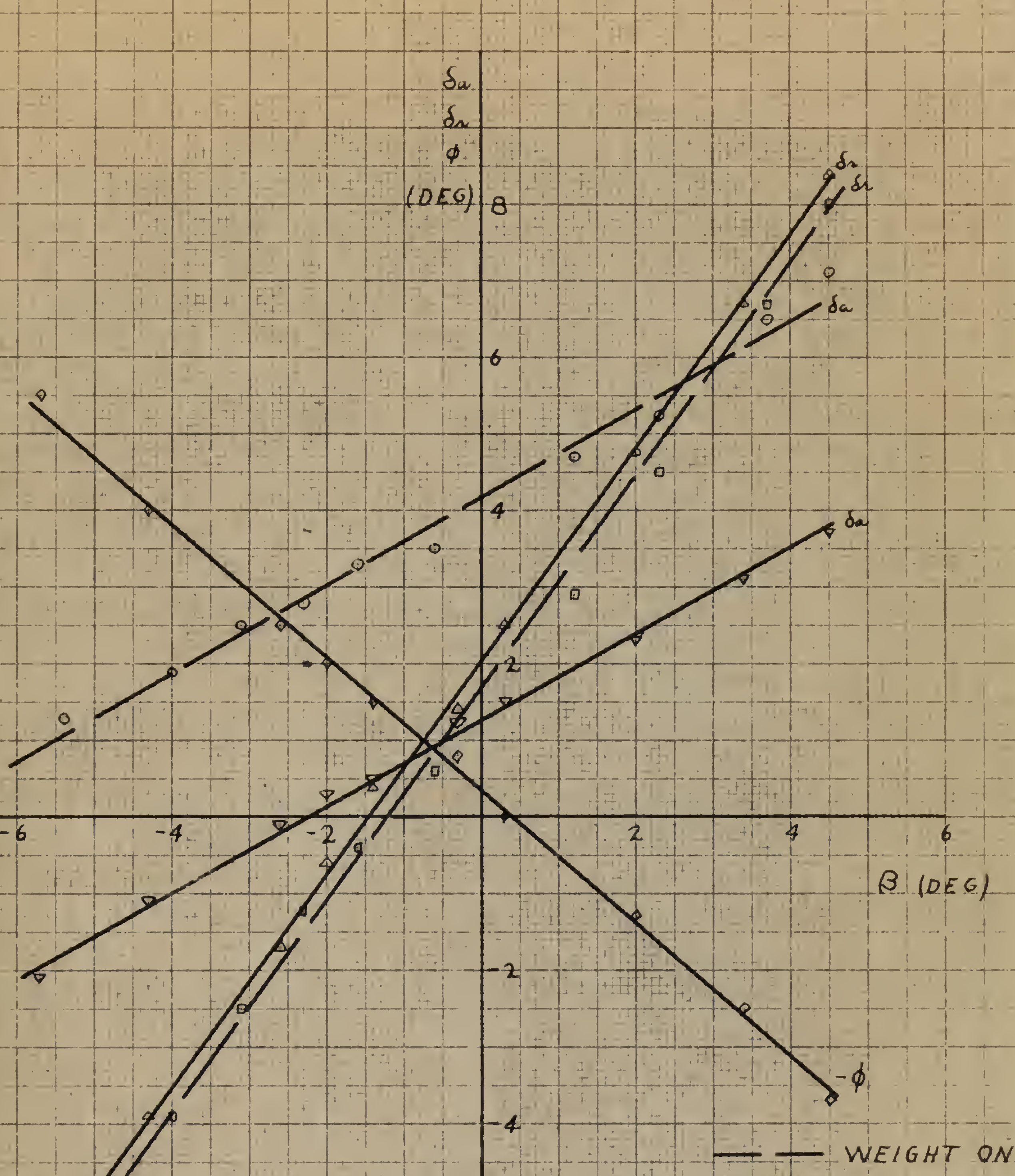

FIG 14
STRAIGHT SIDESLIP
ASSYMETRIC WEIGHT
ON LEFT WING
V=120 MPH (MAX. CONT. POWER)

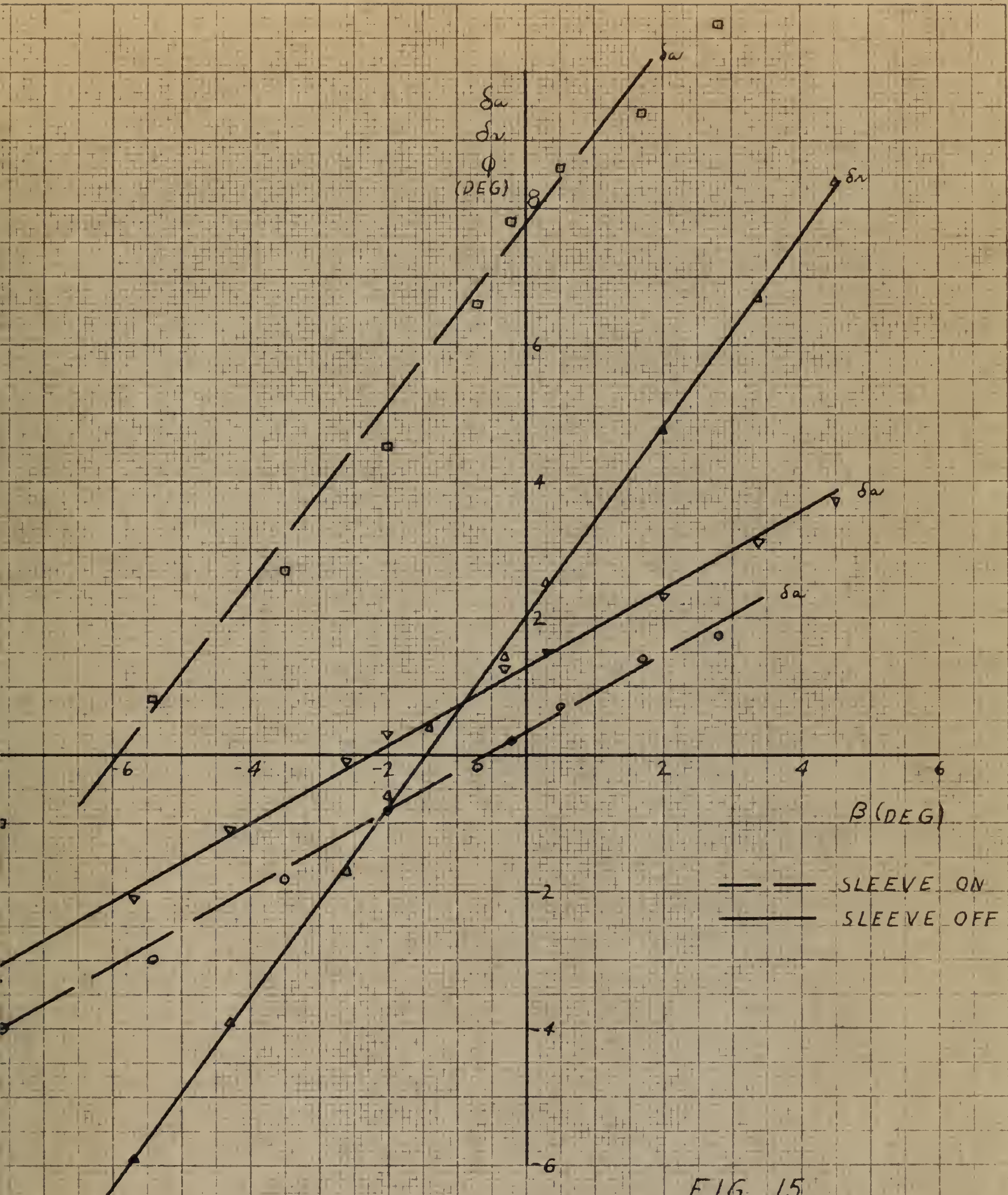

FIG 15
STRAIGHT SIDESLIP
ASSYMETRIC DRAG ON RIGHT WING
V=120 MPH (MAX CONT. POWER)

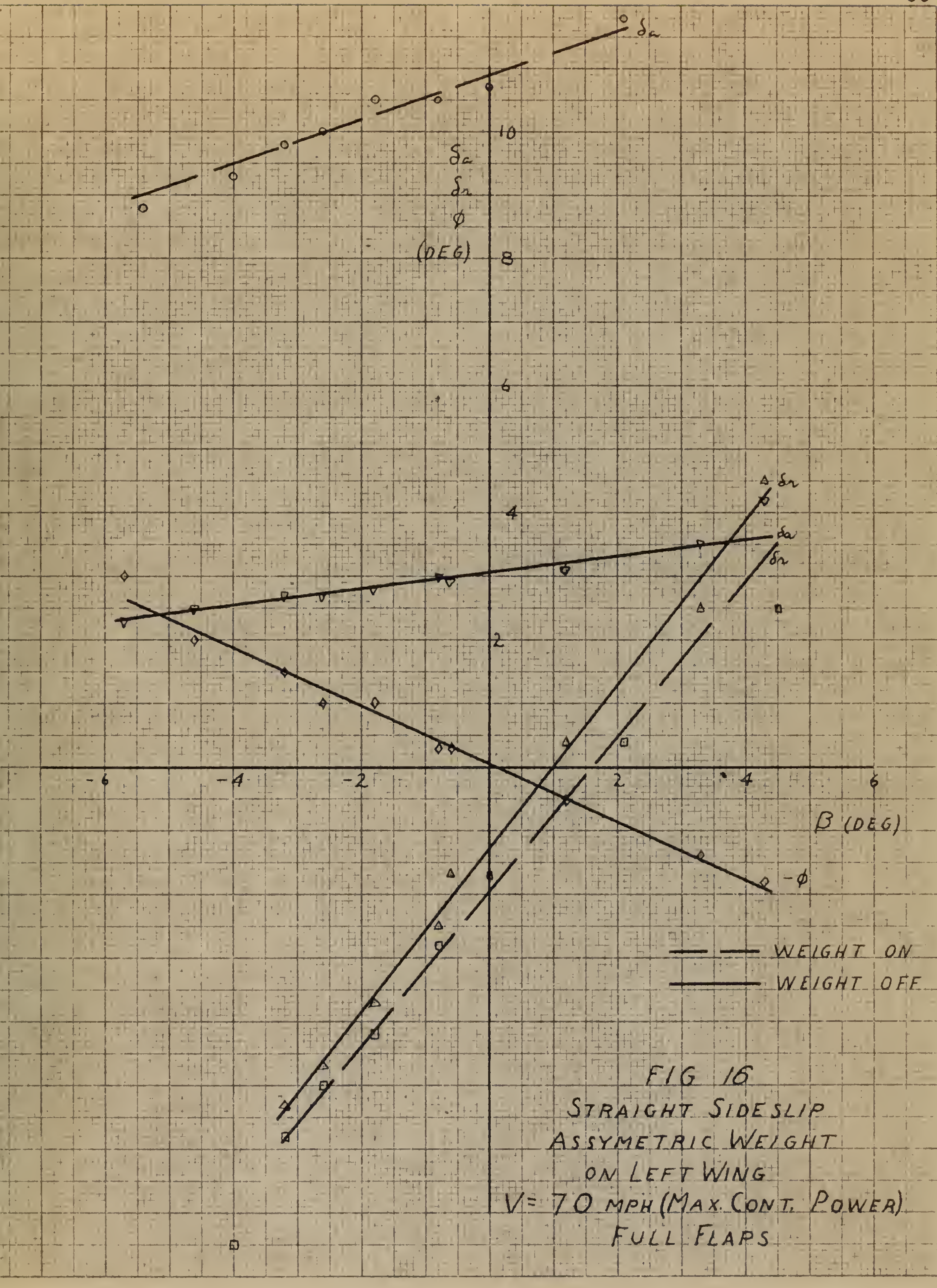

FIG 16
STRAIGHT SIDESLIP
ASSYMETRIC WEIGHT
ON LEFT WING
V = 70 MPH (MAX. CONT. POWER)
FULL FLAPS

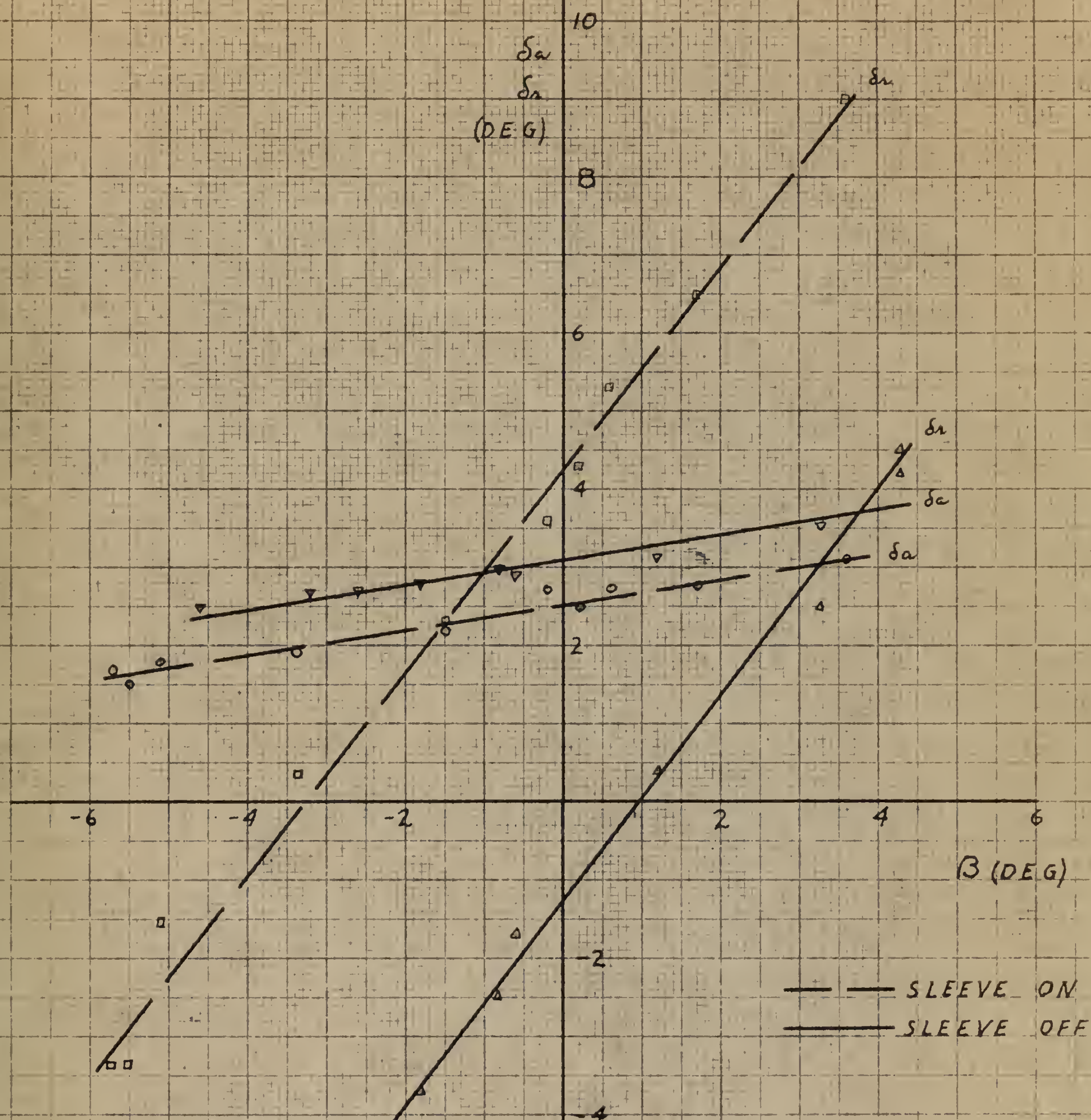

FIG 17
STRAIGHT SIDESLIP
ASSYMETRIC DRAG
ON RIGHT WING
V= 70 MPH (MAX CONT POWER)
FULL FLAPS

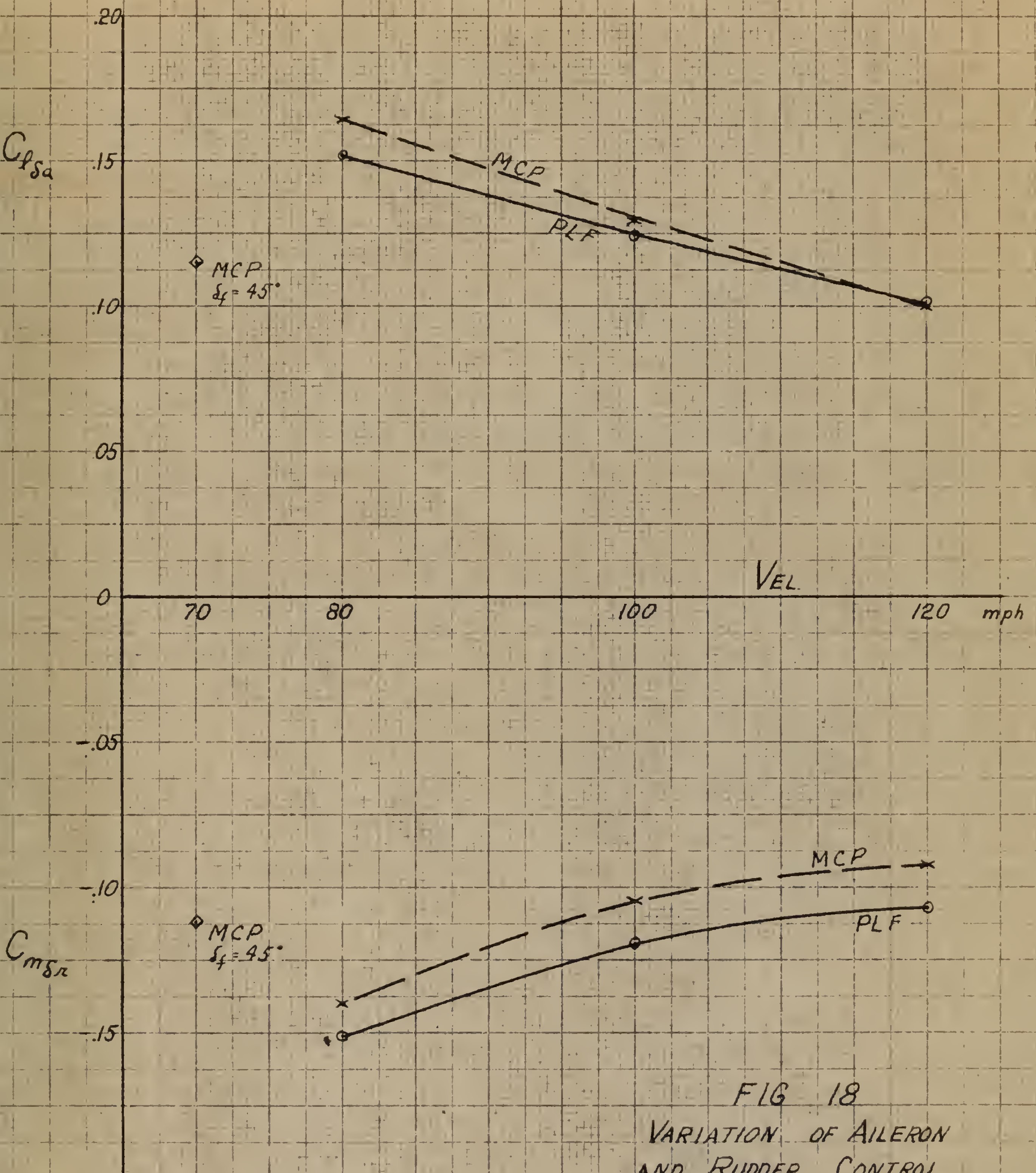

FIG 18
VARIATION OF AILERON AND RUDDER CONTROL POWER WITH VELOCITY

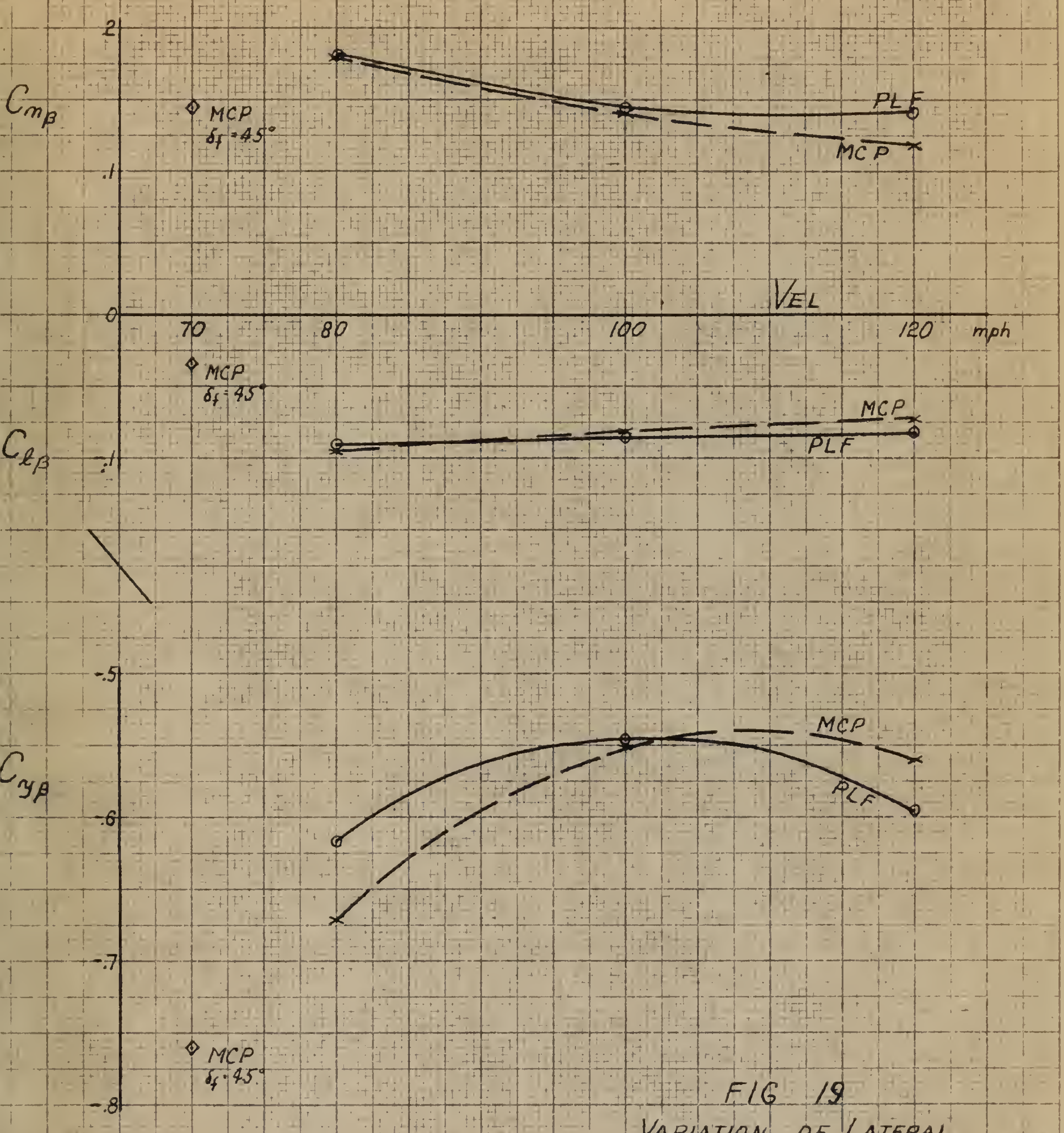

FIG 19
VARIATION OF LATERAL AND DIRECTIONAL STABILITY DERIVATIVES WITH VELOCITY